

## Noninvasive Temperature Imaging Using Diffusion MRI\*

J. DELANNOY, ‡†§ CHING-NIEN CHEN, ‡ R. TURNER, ‡  
R. L. LEVIN, ‡ AND D. LE BIHAN¶

‡Biomedical Engineering and Instrumentation Program, Division of Research Services; §Radiation Oncology Branch/COP/DCT; National Cancer Institute; and ¶Diagnostic Radiology Department, Warren Grant Magnuson Clinical Center, National Institutes of Health, Bethesda, Maryland 20892

Received February 1, 1991; revised February 26, 1991

Efficacy and safety considerations for cancer therapy with hyperthermia require accurate temperature measurements throughout the heated volume. We report the use of molecular diffusion, whose temperature dependence is well known. A dedicated hyperthermia applicator was built, combining a MRI gradient coil and a rf coil. Diffusion and derived temperature images were obtained with a  $1 \times 2$  mm pixel size on a polyacrylamide gel phantom using a clinical 1.5-T whole body MRI system. Temperatures determined from these images using  $1 \text{ cm}^2$  regions of interest were found to be within  $0.2^\circ\text{C}$  of those recorded from the thermocouples and fiber-optic probes placed inside the gel. © 1991 Academic Press, Inc.

### INTRODUCTION

There has been an accumulation of encouraging early biological and clinical evidence to support the view that in association with chemo- or radiotherapy, hyperthermia (HT) may help in the treatment of some human cancers (1). However, the clinical use of deep-seated HT treatment is limited, mainly due to a lack of temperature control (2). Indeed, the effectiveness of HT treatments depends upon reaching at least  $42^\circ\text{C}$  in the tumor, while safety considerations limit the maximum temperature permissible in normal, healthy tissues ( $<42^\circ\text{C}$ ). Therefore, temperature should be monitored throughout the heated region, with at least 1 cm spatial resolution and  $1^\circ\text{C}$  sensitivity. Temperature can be measured very accurately ( $<0.1^\circ\text{C}$ ) with thermosensors such as thermocouples, thermistors, or fiber-optic probes, which can be implanted in heated tissues. These probes are, however, invasive and may be painful and hazardous, so that only few probes can be used under clinical conditions, limiting thus the volume to be investigated. Recently, several noninvasive temperature monitoring methods have been introduced, mainly based on infrared or microwaves, but none of them satisfactorily fulfills the above-mentioned HT requirements (3).

Magnetic resonance imaging (MRI) has been also proposed for monitoring temperature during hyperthermia due to the sensitivity to temperature of some physical

\* Presented at SMRM Workshop on Future Directions in MRI Diffusion and Microcirculation, Bethesda, MD, June 7 and 8, 1990.

† Present address: Sonotron-Hitachi, 91967, Les Ulis, France.

parameters currently MRI accessible, essentially T1 (4–6). MRI also has the potential of monitoring blood flow at the capillary level (7–9), which is a key parameter in the effectiveness of clinical hyperthermia. Unfortunately, the relationship between T1 and temperature is not simple, mainly due to the multifactorial nature of T1. Furthermore, accurate measurements of T1 from MR images are difficult to make. The use of molecular diffusion of water as a thermal indicator to measure and image temperature has been recently suggested (10), on the basis of the direct relationship between temperature and diffusion coefficients which quantify thermal Brownian motion. We have built a dedicated clinical HT device including a MRI rf coil and a Z gradient coil and tested it in a 1.5-T whole body clinical MRI unit.

#### THEORY

##### *Relation between Temperature and Diffusion*

On the basis of the Stokes–Einstein relationship between viscosity and the translational self-diffusion coefficient  $D$ , the following temperature dependence of  $D$  can be used

$$D \propto \exp(-E_a/kT), \quad [1]$$

where  $k$  is Boltzman's constant and  $E_a$  is the activation energy for translational molecular diffusion. Temperature changes thus induce viscosity and diffusion coefficient changes which can be calculated for instance from differentiation of Eq. [1] assuming small or linear variations of  $E_a$  with  $T$  (10):

$$dD/D = (E_a/kT)dT/T. \quad [2]$$

From Eq. [2], it is obvious that temperature changes may be detected from diffusion coefficient measurements.

#### MR IMAGING OF MOLECULAR DIFFUSION

Diffusion coefficients were measured and imaged using a diffusion imaging sequence (11). A map of temperature  $(T)_{x,y}$  can be deduced from the two diffusion images  $D_{x,y}$  and  $D_{0,x,y}$  one obtained at the reference temperature  $T_0(D_{0,x,y})$ , and one obtained at a different temperature  $T(D_{x,y})$ , such that

$$(1/T)_{x,y} = (1/T_0)_{x,y} - (k/E_a)\ln(D/D_0)_{x,y}. \quad [3]$$

In a HT experiment,  $T_0$  is the local tissue temperature before heating, while  $T$  is the local tissue temperature during heating. Using measured values of  $E_a$  (0.18 eV) (10) it appears that sensitivity of temperature mapping from diffusion measurements is somewhat high, since a 1°C change in temperature produces a 2.4% change in the diffusion coefficient.

#### MATERIAL AND METHODS

We used a 1.5-T whole body MRI system (Signa, General Electric) working at 64 MHz in combination with a dedicated hyperthermia applicator. A mini-annular-phased

array (MAPA) radio-frequency HT applicator which had previously been designed to treat limb tumors (12) has been modified and combined with a MRI coil and a Z gradient coil (Fig. 1). The MAPA frame has been reduced to 25 cm in outer diameter and 30 cm in length. Four axially oriented, double, trapezoidally shaped dipole antennas are evenly spaced on the frame's internal circumference. The antennae are constructed from very thin ( $30\ \mu\text{m}$ ) copper film in order to minimize eddy currents during gradient switching. All ferromagnetic components contained in the original design were eliminated. Typically, the dipoles of the MAPA are activated at a single frequency with signals of equal amplitude and phase in order to maximize the energy deposition at the center of the applicator. However, it is possible to vary the MAPA's SAR pattern by activating each dipole using rf signal differing in frequency, phase, and/or amplitude. A single working frequency of 168 MHz was chosen to simplify the construction of the appropriate baluns and filters. To maximize the coupling between the MAPA and the volume being heated (i.e., to achieve a good "match") and to enable surface cooling, a fluid-filled deformable plastic bolus is used to fill the space between the dipole arrays and the limb. Each antenna is balanced with a 168 MHz, 1/4, bazooka-type balun which is linked to a 1:4 power divider. The MAPA was fed via a 50-Ohm power line including a p section filter that rejected 64 MHz with no significant attenuation at 168 MHz, thereby effectively preventing the MRI rf pulses from damaging the HT electronic equipment and ensuring that no interference reached the MRI receiver. All equipment for HT system was positioned outside the screened room.

The applicator includes a modified Alderman-Grant (13) coil used for both transmitting and receiving. The large electric fields generated by the MAPA can capacitively couple to the MRI coil. Thus the MRI receiver had to be protected with a  $\pi$  filter, similar to that described above, which rejected 168 MHz while giving negligible attenuation at 64 MHz. Although this system protected the MRI preamplifier against damage, it could still be saturated during heating, making imaging impossible. Since further filtering would have degraded the MR unit's signal to noise ratio, it was therefore

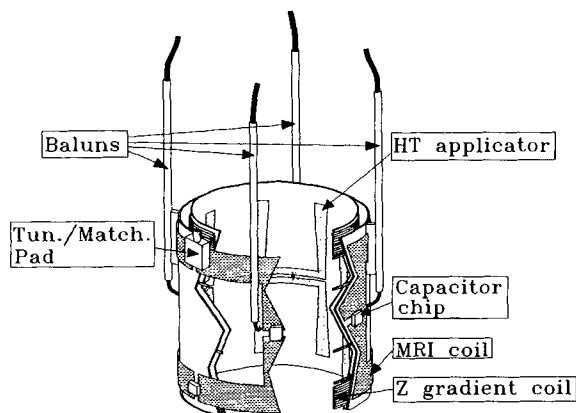


FIG. 1. Design of the dedicated hyperthermia applicator which combines a mini annular phased array, a MRI coil, and a z gradient coil.

necessary to heat and image in a time-sharing manner. The total heating/imaging cycle was set to a 700-ms repetition time (TR), which corresponded to a 500-ms heating period during the "dead time" of each acquisition cycle. In this way, imaging and heating could be achieved efficiently with no time wasted. The MAPA's bolus fluid was supplied via a closed circuit pumping system. Since MRI is very sensitive to overall movements of the object to be imaged, a paramagnetic solution of manganese chloride (1 mM/liter) was used. The manganese chloride decreased dramatically the bolus fluid's relaxation time so that, with the appropriate imaging sequence, the signal coming from the bolus was negligible compared to that coming from the phantom. Because the bolus fluid was not visible in diffusion derived-temperature images, it could be circulated during imaging.

A small  $z$  gradient was included in the combined HT-MRI unit and used instead of the regular body  $z$  coil of the MRI unit. This low impedance coil allowed larger gradient strengths to be reached (40 mT/m) with a shorter rise time ( $<200 \mu\text{s}$ ) without visible eddy currents effects, and thus improved diffusion sensitivity.

The complete HT-MRI system was tested using a dummy leg phantom. This phantom consisted of a 12-cm internal diameter, 60-cm long Plexiglas tube filled with polyacrylamid gel (92.5% water) doped with copper sulfate (5 mM/liter). Eleven Teflon catheters (2 mm o.d.) were also placed longitudinally, 1 cm apart, within the gel, permitting us to insert thermal probes. Invasive temperature measurements were made using fiber-optic probes or thermocouples. Later, hyperthermia sessions were performed on the phantom. During these simulated hyperthermia sessions, the MAPA cooling was adjusted to obtain a temperature of about  $15^{\circ}\text{C}$  within the bolus. The phantom was initially heated with 300 W of rf power for 30 min and then reduced to 100 W to maintain a steady state. A diffusion image was recorded over a time period of 3.5 min. A temperature image was then computed immediately using the MRI's processing system.

## RESULTS

The compatibility of the MAPA with the MRI systems was confirmed by obtaining images which were recorded using pulse sequences sensitized to rf and magnetic field inhomogeneities (e.g., gradient-echo). No artifacts or other distortions were found.

Using Eq. [3], a temperature image was computed in quasi real time from steady state diffusion images recorded before and during a heating (Fig. 2). The pixel size was  $2 \times 1 \text{ mm}$  ( $128 \times 256$  pixels) and the slice thickness was 10 mm. Temperature profiles were recorded from ROIs 1 cm wide and 11 cm long on both sides of the catheter plane. The mean of these measurements, recorded symmetrically every centimeter along the two ROI profiles, together with the temperatures recorded by the probes within the catheters, which were spaced 1 cm apart, can be seen in Fig. 3. The correlation between our noninvasive and invasive temperature measurements was better than  $0.2^{\circ}\text{C}$ .

## DISCUSSION

These experiments demonstrate the ability of MRI to measure temperature changes using molecular diffusion imaging and of combining MRI and HT. Temperature

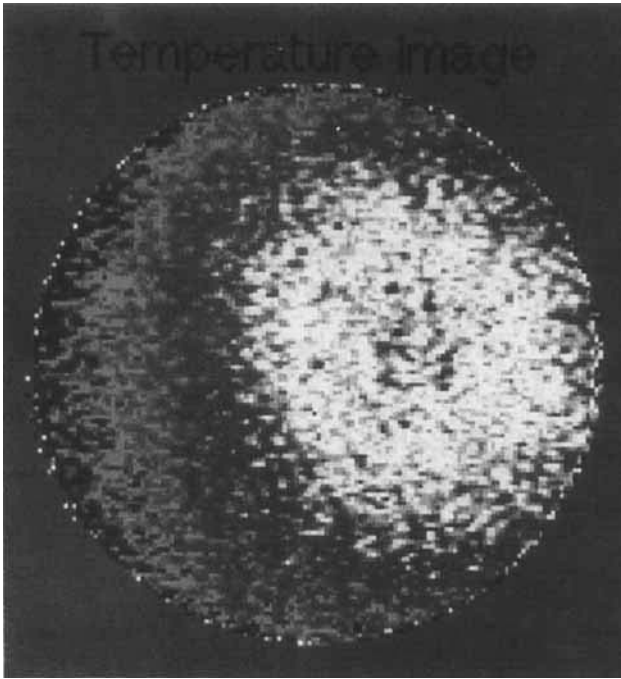


FIG. 2. Temperature image calculated from two diffusion images obtained at room temperature and after heating. Brightness is directly proportional to temperature.

mapping can be achieved three-dimensionally in multislice mode and fulfills the hyperthermia requirements ( $1^{\circ}\text{C}/\text{cm}$ ).

The sensitivity of the temperature determination using diffusion appears to be larger (by a factor of 2) than that of procedures using T1. The acquisition time needed in these experiments ( $2 \times 3.5$  min) is short enough for real-time temperature mapping since thermal changes are slow during hyperthermia. Much shorter acquisition times could be achieved using recently developed fast diffusion imaging techniques such as echo-planar imaging (EPI) (14). Another benefit of these fast imaging methods would be to decrease the sensitivity of diffusion imaging to motion artifacts. Furthermore, the use of Eq. [2] for temperature measurement assumes that the activation energy has been previously determined in biological tissues and that  $E_a$  is constant or varies linearly in the temperature range used for clinical hyperthermia. Previous studies (15) showed that, over a temperature range from  $35^{\circ}\text{C}$  to  $42^{\circ}\text{C}$ , the activation energy  $E_a$  of intracellular water was close to that of pure liquid water. Above  $42^{\circ}\text{C}$ , irreversible changes may occur in some tissues (brain) which could reflect irreversible biological HT damage (15).

Finally, only a map of the temperature change is obtained by this method. If one wants to determine the absolute temperature after heating, the initial absolute temperature must obviously be known. A possible solution in the case of clinical hyper-

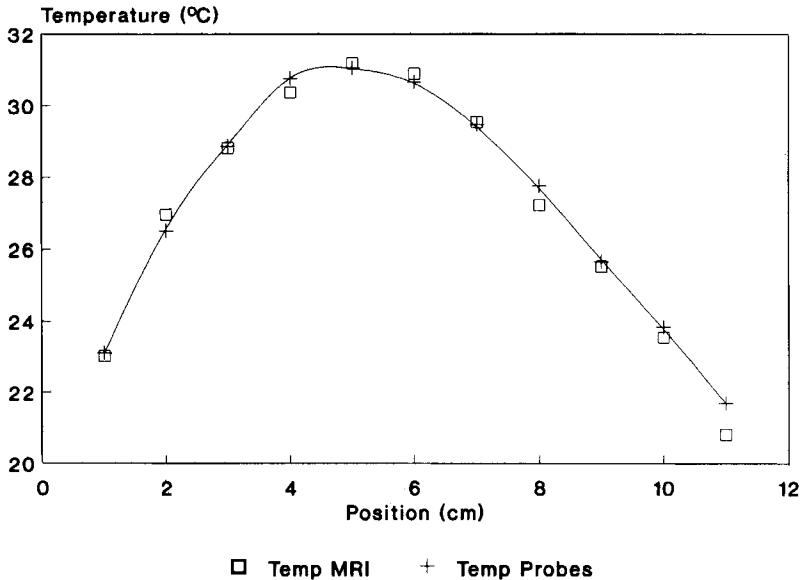


FIG. 3. Plot of the temperature recorded with thermal probes and calculated from the diffusion images within the phantom after heating.

thermia would be to bring the region to be treated to a known uniform temperature by surrounding it with a water bolus at the body temperature.

Furthermore, diffusion coefficient measurements may be affected by other intravoxel incoherent motions of water present in biological tissues. In particular, separation of the contribution of diffusion from that of blood microcirculation may be achieved using additional gradient pulses (8).

On the other hand imaging of perfusion itself may be very useful in hyperthermia studies, since blood circulation plays an important role in the thermal clearance of normal and abnormal tissues. If the change of  $E_a$  in biological tissues was confirmed to be correlated to hyperthermia tissue damage, this could allow evaluation of the treatment efficacy after every hyperthermia session.

#### ACKNOWLEDGMENT

The authors are grateful to Dr. David Hoult for his valuable help and advice.

#### REFERENCES

1. G. M. HAHN, in *Hyperthermia and Cancer* (F. F. Becker, Ed.), 2nd ed. Plenum, New York, 1982.
2. T. C. CETAS, *Cancer Res.* **44** (suppl) 4805 (1984).
3. F. A. GIBBS, M. D. SAPOZINK, AND J. R. STEWART, in *Hyperthermic Oncology* (J. Overgaard, Ed.), 1st ed., Vol 2, p. 155, Taylor and Francis, Philadelphia, 1984.
4. B. KNUTTTEL AND H. P. JURETSCHKE, *Rec. Results Cancer Res.* **101**, 109 (1986).
5. D. L. PARKER, V. SMITH, P. SHELDON, L. E. CROOKS, AND M. FUSSEL, *Med. Phys.* **10**, 321 (1983).
6. R. J. DICKINSON, A. S. HALL, A. J. HIND, AND I. R. YOUNG, *J. Comput. Assist. Tomogr.* **10**, 468 (1986).

7. C. B. AHN, S. Y. LEE, O. NALCIOGLU, AND Z. H. CHO, *Med. Phys.* **14**, 43 (1987).
8. D. LE BIHAN, E. BRETON, D. LALLEMAND, M. L. AUBIN, J. VIGNAUD, AND M. LAVAL JEANTET, *Radiology* **168**, 497 (1988).
9. I. R. YOUNG, A. S. HALL, D. J. BRYANT, *et al.*, *J. Comput. Assist. Tomogr.* **12**, 721 (1988).
10. D. LE BIHAN, J. DELANNOY, AND R. L. LEVIN, *Radiology* **171**, 853 (1989).
11. D. LE BIHAN, E. BRETON, D. LALLEMAND, P. GRENIER, E. A. CABANIS, AND M. LAVAL JEANTET, *Radiology* **161**, 401 (1986).
12. J. L. GUERQUIN-KERN, H. J. HAGMAN, AND R. L. LEVIN, *Med. Phys.* **14**, 674 (1987).
13. D. W. ALDERMANN AND D. M. GRANT, *J. Magn. Reson.* **36**, 447 (1979).
14. R. TURNER, D. LE BIHAN, J. MAIER, R. VAVREK, L. K. HEDGES, AND J. PEKAR, *Radiology* **177**, 407 (1990).
15. D. LE BIHAN, J. DELANNOY, R. L. LEVIN, J. PEKAR, AND O. LEDOUR, in "Proceedings of the Society of Magnetic Resonance in Medicine 8th Annual Meeting, 1989," 141.